ELECTROLUMINESCENCE IMAGING OF PV DEVICES: SINGLE-TIME-EFFECT STATISTICS AND REMOVAL

K.G. Bedrich*, M. Bliss, T.R. Betts, R. Gottschalg
Centre for Renewable Energy Systems Technology (CREST), Wolfson School Mechanical, Electronic and Manufacturing Engineering, Loughborough University, Loughborough, Leicestershire, LE11 3TU, UK
*Corresponding Author K.Bedrich@lboro.ac.uk

ABSTRACT: The statistics and removal of occurring specific image artefacts (i.e. single-time-effects [STE]) during qualitative analysis of EL imaging is discussed. STE are caused by single nuclear particles such as heavy ions, along with neutrons and protons with energies above 10 MeV. When charged particles cross the sensitive region of the CCD matrix, they cause effects of ionization and lead to spots only visible once after signal readout. Depending on whether STE occur in the EL image with sample excitation or in the background image without, they are visible in the corrected EL image as bright or dark spots. These can be confused conceivably with cell defects. Within this work the intensity offset due to STE as well as their occurrence over time is evaluated for multiple EL images. For the examined setup it is shown that the disruptive influence of STE is visible for measured cell voltages under 0.65 V. For this case a robust STE removal method is proposed using an additional EL image taken in series.

Keywords: Electroluminescence, Devices, Calibration, Image quality, Evaluation

1 Introduction

Single-time-effects (STE) as defined in [1] are caused by 'single nuclear particles such as heavy ions, along with neutrons and protons with energies above 10 MeV'. While the charged particles cross the sensitive region of the CCD matrix effects of ionization lead to spots only visible once after signal readout. They can be seen as a single imaging fault. STE can be identified as small spots or straight to curvy lines and potentially can be cunfused with eg. micro cracks or shunts (Figure 1). They can be differentiated from hot pixels [2] by comparing two images taken in series with the same exposure time. While hot pixels will remain fixed in place and intensity, the propability of STE to occur twice at the same time is neglibible. STE saturate CCDs bit by bit. For space-borne CCDs Hill et al. reported that an exposure time of 1000s would affect already 2.5% of the image [3].

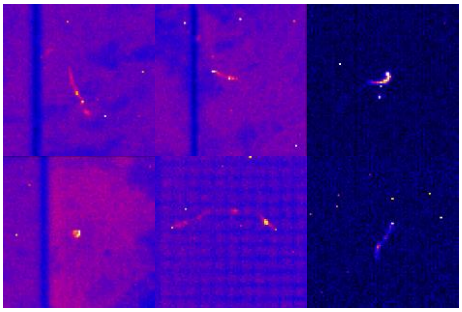

Figure 1: Selection of STE with different size and intensity. Hot pixels are visible as single bright pixels.

However, statistics quantifying the severity of this effect are to date not reported for EL imaging on PV devices.

2 STE Measurement and Statistics

The following analysis describes the visibility of STE to be seen in one specific cell of a 4x9 cSI PV module (Figure 2). The results dependend on the camera, the PV device and the EL imaging setup. For the examined setup, 116 background images were used. The images were taken with a SensoCam HR-830 between 14/04/2015 and 08/05/2015. An image mask M_{STE}, marking the position of STE, was than created as follows:

1. Select image pair (two images i_0, i_1 taken in series at the same exposure time)
2. Determine the noise level function *NLF* (standard deviation over pixel intensity) as described in [4].
3. Calculate the image difference:
$$I_d = i_0 - i_1$$
4. Create a STE free template image from the local minimum:
$$I_{min} = \min(i_0, i_1)$$
5. Mask STE (M_{STE}) as all pixel indices where the difference of both images excedes the local noise level set as:
$$M_{STE} = I_d > 4 \cdot NLF(I_{min}) \quad (1)$$
6. In order to remove image noise from M_{STE}, remove all pixels without neighbours. This method can also remove STE only built by one pixel. However their number will be

small in relation to otherwise remaining noise.

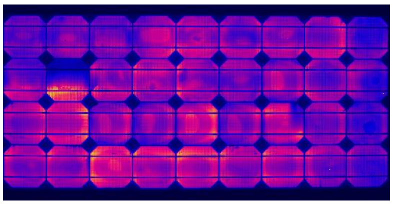

Figure 2: EL setup, used for statistical analysis on STE

The number of STE was calculated as the number of spatially connected clusters within M_{STE} and can be seen in Figure 3a for different exposure times. As expected the number of STE increases linearly with time. The average STE size was determined as the number of positive elements in M_{STE} divided by the number of STE found. This is displayed in Figure 3b. The distribution of different STE sizes narrows down for an increasing exposure time because of the likewise increasing number of STE which average the result.

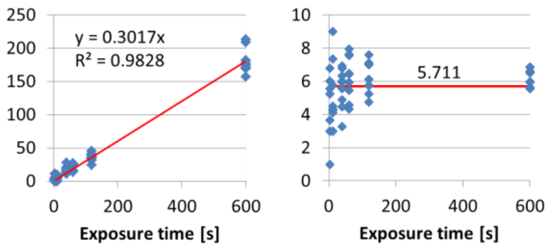

a) Number of found STE b) STE size [pixels]

Figure 3: STE development over exposure time

A probability density function of the STE pixel intensity PDF(STE) was taken from the difference image I_d at all STE positions M_{STE} and averaged for all image pairs. The result (Figure 4) shows that the PDF can be approximated by an unbounded Johnson SU distribution (JSU), a transformation of the normal distribution. JSU was chosen as the best fit among 82 continuous distributions within the scipy.stats package [5].

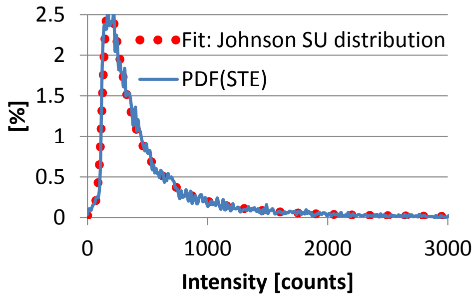

Figure 4: Blue: Probability density function (PDF) of STE over pixel intensity; Red dots: Fit of the PDF using a Johnson SU distribution

Using the ascent and average STE size (Figure 3) as well as the ratio PV cell size over image size it is possible to quantify the probability of one STE to be found in a specific cell of the DUT (Figure 5). The plotted blue line indicates that on average every cell will have one STE at exposure times longer than 200s. Given that many EL images are taken with longer exposure times, this would mean that many effects identified from single images may actually be STE.

This is remarkable because this module EL measurement needed an exposure time of 600s to generate an averaged signal-to-noise ratio of 61 or respective 60s for 6.1 (measured using the averaged SNR method described in [6]). STE increase the intensity of affected pixels. Therefore depending on whether STE occur in the EL or the background image they are visible in the background corrected EL image as bright or dark spots. The visibility of STE (and other features) depends on the relative intensity difference. The threshold of visibility was found to be independent from the image intensity under well-lit (photopic) conditions according to Webers law [7]:

$$\frac{\Delta I}{I} = constant \sim 1\% \qquad (2)$$

The visibility of STE in Figure 5 (red lines) is quantified for three different probabilities which can be explained as follows. The '50x50%' case marks the probability of an STE with average intensity over an average EL signal. In contrast to this the '1x1%' case compares the effect on an STE within the highest one percent of the PDF (Figure 4) to the darkest 1 % of a Gaussian distributed EL signal. This case is considered as the worst case scenario. The resulting ratios are indirect because the STE intensity remains constant while the EL signal increases linearly over time.

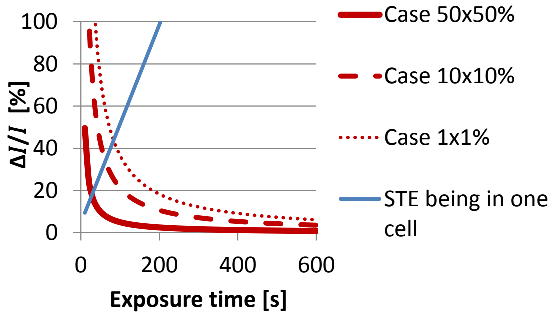

Figure 5: Red: Intensity ratio (STE/EL) for three different cases; Blue: Probability of one STE to be found in one specific cell in the module

Figure 5 can be interpreted as follows: After 200s on average every cell will have one visible STE. At this time for the case '10x10%' the intensity ratio between STE and EL signal will be 10% or higher. This is enough to be misinterpreted as shunt or micro-crack. However, due to the small average size of ~6 pixels, STE will be often too small to lead to wrong conclusions.

Although the probability of STE occurrence increases linearly with exposure time, their intensity distribution remains constant. In consequence, Figure 6 shows the minimum EL induced intensity increase, needed to not notice 50%, 90%, 99 % of STEs as artefact.

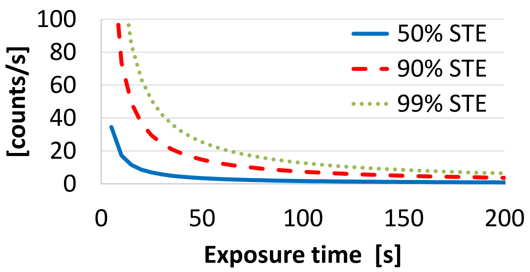

Figure 6: Minimum intensity increase per second of a pixel in an EL image for STE to be invisible according to Equation (2)

For the EL setup used, the median intensity increase was measured for multiple modules at 10% and/or 100% of their rated short circuit current I_{sc}. The injected power at 100% I_{sc} was within 4-450W. In order to plot these different rated modules together a 'quasi' cell voltage V_{cell^*} was calculated, neglecting series resistance as:

$$V_{cell^*} = \frac{V_{mod}}{n_{cells}} \tag{3}$$

The result (Figure 7) follows an exponential relationship. This is as expected since the luminescence emission is proportional to $\exp(V_{local})$ [8, 9].

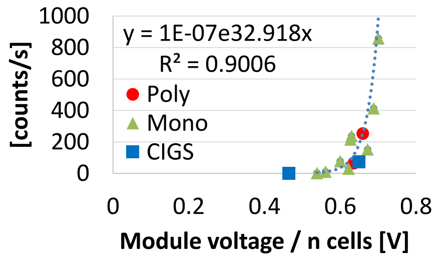

Figure 7: Measured median intensity increase per second for 11 different modules at either 10% I_{sc} and/or 100% I_{sc}

Figure 6 suggests that an intensity increase above 100counts/s would be suitable to make STE unnoticeable for exposure times over 20s. For the devices examined, this intensity increase is on average exceeded for assumed cell voltages above 0.65V (Figure 7).

It is suggested to carry out the STE removal routine below for the following cases:

- Devices below the mentioned voltage,
- Images with long exposure times and low SNR,
- Images to be used for calibration (e.g. flat field and background images).

3 STE Removal

Two EL images taken in series at the same exposure time are needed. An STE mask is calculated, as shown in (1). An average image $I_{avg} = 0.5 * (i_0 + i_1)$ is built. All places identified with STE will be then set to the STE free template image:

$$I_{avg}[M_{STE}] = I_{min}[M_{STE}] \tag{4}$$

The averaging procedure will also increase the signal-to-noise ratio (SNR) for every position, not affected by STE. The SNR will be increased by the following factor when averaging two images with Gaussian distributed noise:

$$f_{avg} = \frac{1}{\sqrt{0.5}} \approx 1.41 \tag{5}$$

As to be seen in Figure 8, the proposed STE removal routine not just removes the influence of STE but also increases the SNR.

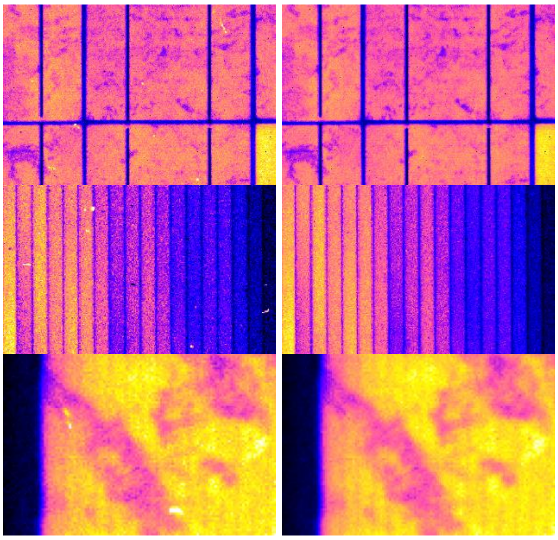

Figure 8: Excerpt of three different EL images, affected by STE before (left) and after (right) STE removal

4 Summary and Conclusion

This paper describes statistics and removal of single-time-effects (STE) caused by cosmic high energy radiation interacting with the CCD cameras sensor. STE are imaging artefacts, which can be confused with cell defects. For the examined EL imaging setup an average STE size of 6 pixels and intensity of 300 counts was observed. With on average one new STE every three seconds, every cell of the PV module, as for the case in Figure 2, would be affected with these image artefacts after an exposure time of 200s.

However, STE remain invisible if the relative intensity difference is sufficiently small. If the EL signal of a PV module increases over 100 counts/s, STE wont be noticed for exposure times higher than 20 sec. For the observed devices a minimum cell voltage (neglecting series resistance) of 0.65V was found to be enough to deliver the required photon flux. For devices with lower voltage STE removal using an additional EL image is proposed. To remain at the same signal-to-noise ratio this method increases the absolute exposure time (ignoring time needed for image capture and processing) about 41%.

References

[1] K. N. Ermakov, N. a. Ivanov, O. V. Lobanov, V. V. Pashuk, M. G. Tverskoy, and S. M. Lyubinskii, “Experimental investigation of the effect of high-energy protons on charge-coupled devices,” *Tech. Phys. Lett.*, vol. 36, no. 7, pp. 610–612, Sep. 2010.

[2] G. R. Hopkinson, C. J. Dale, and P. W. Marshall, “Proton effects in charge-coupled devices,” *IEEE Trans. Nucl. Sci.*, vol. 43, no. 2, pp. 614–627, Apr. 1996.

[3] R. Hill, W. Landsman, D. Lindler, and R. Shaw, “Cosmic ray and hot pixel removal from STIS CCD images,” *Calibration Work.*, pp. 120–125, 1997.

[4] K. G. Bedrich, M. Bliss, T. R. Betts, and R. Gottschalg, “Electroluminescence Imaging of PV devices: Determining the Signal-To-Noise Ratio,” 2016.

[5] “Scipy.stats - Statistical functions,” *The Scipy community*, 2016. [Online]. Available: http://docs.scipy.org/doc/scipy/reference/stats.html.

[6] IEC, “IEC TS 60904-13 PHOTOVOLTAIC DEVICES - Part 13: Electroluminescence of photovoltaic modules - draft.” 2015.

[7] H. R. Wu and K. R. Rao, *Digital Video Image Quality and Perceptual Coding (Signal Processing and Communications)*. Boca Raton, FL, USA: CRC Press, Inc., 2005.

[8] T. Potthoff, K. Bothe, U. Eitner, D. Hinken, and M. Köntges, “Detection of the voltage distribution in photovoltaic modules by electroluminescence imaging,” *Prog. Photovoltaics Res. Appl.*, vol. 18, no. 2, pp. 100–106, Mar. 2010.

[9] C. Karcher and H. Helmers, “Temperaturedependent electroluminescence and voltages of multijunction solar cells,” in *28th European Photovoltaic Solar Energy Conference and Exhibition*, 2013, pp. 107–112.